1995 NASA/ASEE SUMMER FACULTY FELLOWSHIP PROGRAM
JOHN F. KENNEDY SPACE CENTER
UNIVERSITY OF CENTRAL FLORIDA

CRACK GROWTH BEHAVIOR OF AISI-4340 STEEL DURING ENVIRONMENTAL EXPOSURE

Dr. Lucille A. Giannuzzi
Assistant Professor
Department of Mechanical and Aerospace Engineering
University of Central Florida
Orlando, Florida

KSC Colleague - Rupert Lee
Material Science

Contract Number NASA-NGT-60002
Supplement 19

August 9, 1995

ACKNOWLEDGMENTS

I would like to express my sincere appreciation to the 1995 NASA/ASEE Summer Faculty Fellowship Program at Kennedy Space Center for their sponsorship of this research project. In addition, Dr. Ray Hosler, Ms. Kari Stiles, and Mr. Gregg Buckingham also deserve recognition for their administrative efforts throughout the summer, and for keeping the program running smoothly.

I would like to thank all of the members of the Materials Section of the Materials and Chemical Analysis Branch at KSC for stimulating discussions and invaluable help along the way. In particular, I would like to thank my NASA colleague, Dr. Rupert Lee for his guidance throughout the project, Mr. Peter Marciniak, for his help and expertise on metallographic specimen preparation and for enlightening discussions, Mr. Johnny Gay for machining anything on a moments notice, and to Mr. Heri Soto, for a memorable tour of LC-39a.

Specials thanks to Mr. Roger MacDonald, UCF graduate student, for his assistance and diligence on this project.

ABSTRACT

AISI-4340 is observed to undergo stress corrosion cracking when subjected to a constant load during exposure to a 3.5% NaCl solution. Crack initiation, nucleation, and growth has been monitored as a function of time. Stepped regions consisting of fast and slow crack growth periods are shown to correspond to microstructural changes observed in the fracture surface of the steel. These regions of fast and slow crack rate variations with time show that the crack growth rates do not increase continuously with an increase in the stress intensity.

SUMMARY

Compact tension specimens have been used to assess the stress corrosion cracking behavior of a high strength AISI-4340 steel. The crack tip was wet with a 3.5% NaCl solution and pulled in tension at a constant load until failure. The crack mouth opening displacement, the crosshead displacement, and the test duration was continuously monitored. Due to the plane stress conditions which were present during testing, K_{Iscc} and K_{Ic} could not be determined from this study. The crack initiation, nucleation, and growth rates may appear either as a gradual transition as time progresses until failure, or may yield a stepped behavior as time progresses. When a stepped behavior is observed, crack growth rates fluctuate between fast and slow values as K increases, which is not consistent with prior observations where the log(crack growth rate) increases continuously as K increases. Preliminary microstructural analyses of specimen fracture surfaces shows evidence of changing crack growth morphology in regions which are believed to correspond to the stepped crack growth behavior.

TABLE OF CONTENTS

LIST OF FIGURES

ABBREVIATIONS AND ACRONYMS LIST

a	crack length
B	C(T) specimen thickness
C(T)	compact tension specimen
CMO	crack mouth opening
E	Young's modulus
E'	effective Young's modulus
F	geometric constant
F'	geometric constant
HCL	hydrogen chloride
HRC	hardness Rockwell C-scale
K	stress intensity
K_{Ic}	critical stress intensity
K_{Iscc}	critical stress intensity for the onset of SCC
LEFM	linear elastic fracture mechanics
NaCl	sodium chloride
SCC	stress corrosion cracking
SEM	scanning electron microscope (microscopy)
UTS	ultimate tensile strength
W	length of a C(T) specimen from the load axis
YS	yield strength
α	the ration of a/W
ν	Poison's ratio
π	pi (3.14....)
σ	applied stress
σ_y	yield stress

I

INTRODUCTION

Environmental cracking or stress corrosion cracking (SCC) of a material is the result of a synergistic effect of exposure to a corrosive environment while under stress (i.e., a tensile stress). The combination of the environment and a tensile stress acting on a material is more deleterious than either the effect of the environment, or the effect of stress, acting alone. Thus, brittle catastrophic failure may occur in structural components in the presence of a corrosive environment even if the applied stresses are well below the yield strength of the material. The threat of SCC failures at NASA-KSC is a major concern for the shuttle and ground support materials due to the corrosive environment that these structural materials are subjected to. For example, the shuttle launch pads are located only 2500 feet (762 m) from the Atlantic Ocean, and a shuttle launch spews HCl as a by-product of the solid rocket booster combustion process. The abundance of chloride ions allows for the tremendous potential for corrosion failures on and around the launch facilities. Hence, it is very important to understand SCC mechanisms, so that materials selection and structural design can be incorporated into this harsh environment.

Structural materials are seldom loaded in a static condition. In addition, environmental conditions usually fluctuate. That is, structural materials are usually exposed to both cyclic loading conditions as well as cyclic environmental wet and dry periods. The ultimate goal of this project is to evaluate the effect of cyclic loads and exposures on AISI 4340 steel. However, the incubation and nucleation of crack growth during static loading and constant environmental exposure must first be understood.

The relative influences of electrochemical and mechanical factors in the corrosion and SCC damage of a material is shown in the crack growth vs. time curve in figure 1(ASM 1987). There exists an incubation and nucleation time period for crack growth which is primarily driven by electrochemical driving forces. Then, as time progresses, the driving force for crack growth leans toward the mechanical factor in the system. There is no accepted model for this particular crack growth phenomenon. That is, either a gradual transition of crack growth may occur until specimen failure as in figure 1, or, repeated succession of short steps of initiation and growth may occur until specimen failure.

The path of cracking in high strength steels is intergranular along prior austenite grain boundaries (Phelps and Loginow, Davis, and Dean and Copson). Mixed inter- and transgranular cracking has been observed in 4340M and 4330 steel (Davis et al.). In AISI 4340 steel, stress corrosion fracture surfaces were characterized as surface nucleated, intergranular fractures with secondary cracking or deep crevices (Phillips et al.). Transmission electron microscopy on AISI 4340 exposed to a 3% NaCl solution has shown that epsilon carbide precipitates were found to be preferentially attacked (Tiner and Gilpin). The attack was attributed to microstrains an/or depletion of alloying elements from the are adjacent to the carbide.

Linear-elastic fracture mechanics (LEFM) has been used to characterize the mechanical component of the driving force of SCC. The stress intensity, K, is the ability of a material to resist crack growth at an applied stress (i.e., the intensity of stress at the crack tip) and is given by:

$$K = F\sigma\sqrt{\pi a}$$

K = stress intensity (units of MPa $\sqrt{m}$)
a = crack length
σ = applied stress
F = f(geometry, a/W)

For a compact tension C(T) specimen, whose schematic diagram is shown in figure 2:

$$K = F' \frac{P}{W\sqrt{B}}$$

where:

B = specimen thickness
W = length of specimen from the load axis
F' = f(geometry, a/W) and $F \neq F'$

and

$$F' = \frac{(2+\alpha)}{(1-\alpha)3/2}(0.886 + 4.64\alpha - 13.32\alpha^2 + 14.72\alpha^3 - 5.6\alpha^4) \text{ where } \alpha = a/W$$

In order for LEFM to be applicable:

$$a, (W-a), h \geq \frac{4}{\pi}\left(\frac{K_{Ic}}{\sigma_y}\right)^2$$

where h = distance from the crack center line to the specimen edge, K_{Ic} is the critical fracture toughness, and σ_y is the yield strength.

For plane strain conditions:

$$B, a, (W-a), h \geq 2.5 \left(\frac{K_{Ic}}{\sigma_y}\right)^2$$

If plane strain conditions do not exist (i.e., plane stress conditions exist), K_{Ic} will be overestimated, because K_{Ic} increases as thickness, B, decreases. Therefore, the critical stress intensity factor should not be determined under plane stress conditions. The crack mouth opening displacement (CMO) is related to the material properties and crack growth as follows:

$$\frac{(CMO)}{P} = \left(\frac{1}{E'B}\right) q(a/W)$$

where q(a/W) = f(geometry, a/W), and E' is the effective Young's modulus (=E for plane stress, = $E(1-\nu^2)$ for plane strain). The crack growth rate is then related to the stress intensity as shown in figure 3 (ASM 1987). In stage I, the crack growth begins at a stress intensity = K_{Iscc} and the crack growth rate increases as K increases. In stage II, the crack growth rate is constant and independent of K and depends on the material/environment interaction. In stage III, the crack growth rate increases as K increases and approaches K_{Ic}.

There are several methods available for evaluating the stress corrosion susceptibility of a material. Each method, of course, has advantages and disadvantages. The method chosen in the present study consisted of constant load, K increasing, conditions. The advantage of these conditions is that they best mimic the loading conditions of structural members. The disadvantage to these parameters is the potentially long duration of each test.

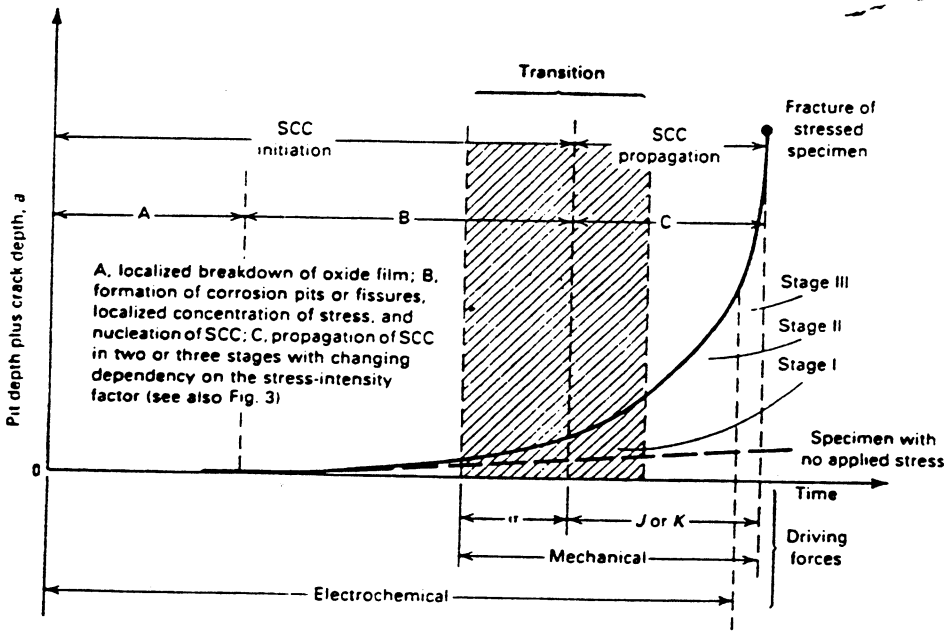

Figure 1. Schematic diagram of SCC crack growth behavior (from ASM 1987).

Compact Tension Specimen

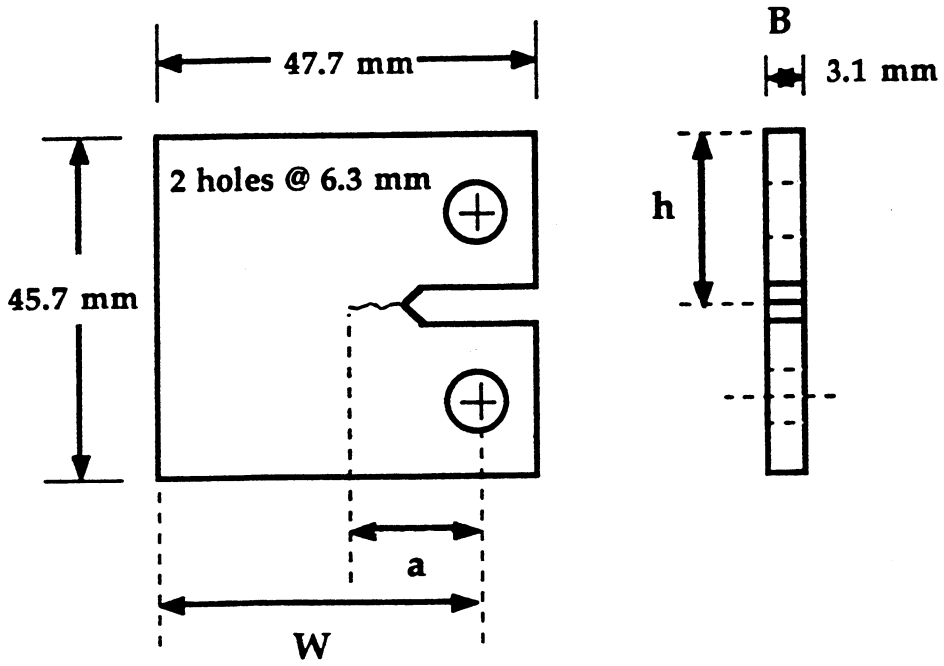

Figure 2. Schematic diagram of the C(T) specimen.

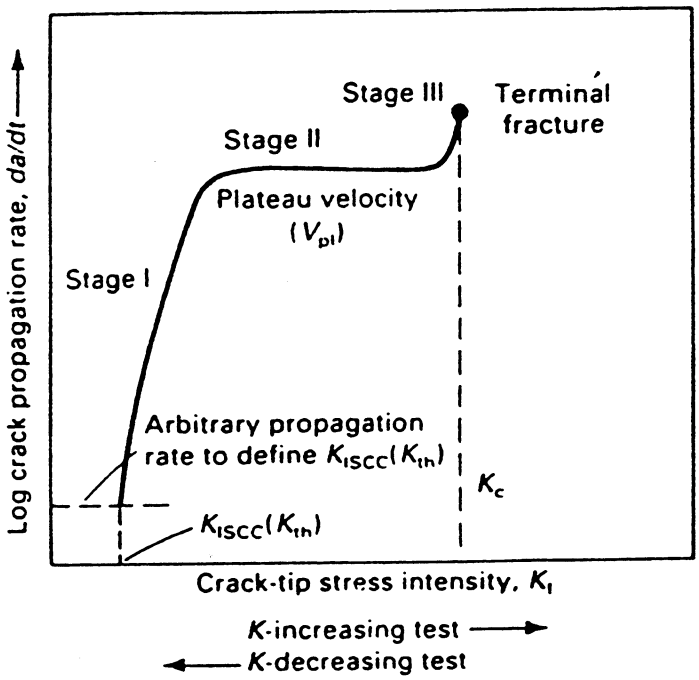

Figure 3. Schematic diagram of crack growth rates as a function of stress intensity (from ASM 1987).

II

EXPERIMENTAL PROCEDURES

The material chosen for this study was AISI-SAE 4340 steel plate of 3.1 mm in thickness. The steel was heat-treated to achieve a Rockwell hardness value of HRC = 42.8 ± 0.7. At least twenty-nine (29) compact tension C(T) specimens were machined from the plate according to ASTM standard E399 (see figure 2). It should be noted that the plate thickness was such that plane stress, and not plane strain conditions, were operating during tension testing. Several material properties of AISI-4340 are listed in Table 1.

Table 1. Properties of AISI-SAE 4340

UTS ~ 1500 MPa

YS ~ 1365 MPa

K_{Ic} ~ 75 MPa $\sqrt{m}$

K_{Iscc} ~ 30 MPa $\sqrt{m}$

Precracks were incorporated into the specimens by fatigue testing on an MTS Hydraulic Tester. Stress corrosion cracking tests were initiated by placing a piece of gauze fabric into the C(T) notch. The gauze fabric was then soaked with a 3.5% NaCl water solution. The C(T) specimen was loaded after a 0.5 hr pre-soak in the NaCl solution. Prior to loading, a clip strain gauge was fastened to the machined knife edges (not shown in figure 2) of the crack mouth of the specimen, so that the crack mouth opening displacement could be monitored throughout the test. The wet gauze remained in the C(T) notch throughout the duration of the test and served as the source of corrosive media. The gauze was replenished with NaCl solution as needed by squirting solution into the notch area using an eye dropper. Constant load tests were performed on a SATEC Universal Testing Machine equipped with the Nuvision II Software Package for automation of the testing. The crack mouth opening displacement, load, and crosshead displacement were monitored as a function of time, for each test. In addition, each test was video monitored and recorded so that an independent method of crack growth rates could be calculated.

The 4340 steel was polished for microstructural analysis using traditional metallographic polishing operations, followed by etching in Nital. Polished and etched surfaces were examined in a LECO metallograph. Macrographs of the C(T) fracture surfaces were obtained using a SONY CGD camera and video printer. Fractography was performed in a JEOL scanning electron microscope (SEM).

III

RESULTS AND DISCUSSION

Light optical micrographs of the microstructure of the 4340 steel are shown in figure 4. As evident from the micrographs, the microstructure of the steel consists primarily of martensite. The region in figure 4a is parallel to the direction of the crack plane, figure 4b shows the microstructure from the plane perpendicular to the crack direction and parallel to the C(T) thickness, and figure 4c shows the microstructure from the front surface of the C(T) specimen. Note that the bar on the micrographs corresponds to 25 μm.

Table 2 summarizes the SCC tests which were performed and lists the specimen identification number, the applied load, in kN, the total change in crack mouth opening displacement after loading (Δ CMO), in (m), and the length of time of each test at load in days, hours, minutes, and seconds. Test specimen 29 was the only specimen listed which did not fail in the time shown. Note that the time to failure does not correspond to the applied load, but depends on the initial applied stress intensity which varied with the initial crack length for each specimen (not listed in table 2).

Table 2. Summary of SCC Test Results

Specimen	Applied Load (kN)	Δ CMO (m)	Time (d:hh:mm:ss)
11	7.8	2.9×10^{-7}	0:01:01:52
13	9.8	1.6×10^{-5}	0:01:06:20
28	5.9	2.5×10^{-4}	0:05:39:36
14	5.9	9.1×10^{-5}	0:06:36:00
07	8.9	3.2×10^{-4}	1:01:00:11
29	5.9	6.4×10^{-7}	1:22:35:24 + (no failure)

The CMO vs. time for each specimen listed in Table 2 are plotted and shown in figures 5-10. Note that only specimen 14 shows a smooth transition from the initiation and nucleation stage of a crack, to crack growth, and subsequent failure. All of the other tests show one or more stepped crack growth arrest periods prior to fast fracture of the specimen. Note that SCC testing of specimen 29 was interrupted and therefore, the test did not result in specimen failure. Due to time constraints, the data could not be presented in the traditional manner which plots the log of the crack growth rate as a function of instantaneous stress intensity (as in figure 3). However, it is evident that as

the crack grows, the stress intensity, K, increases. Thus, while K is constantly increasing throughout the duration of a test, the velocity of the crack may increase or decrease in a stepped fashion as evident by the crack growth arrest periods in figures 5-10. Hence, the traditional stage I, stage II, and stage III portions of the log crack rate vs. K behavior during SCC is only observed for specimen 14 in this study.

The entire fracture surface from specimen 13 is shown in figure 11, and is typical of all of the SCC fracture surfaces which were observed. Extending from right to left, the fracture surface consists of the notch, the fatigue precrack region, the SCC region (darkest area), and the fast fracture region (largest and brightest area showing cleavage).

Fractography was performed on all of the SCC specimens and select SEM micrographs are shown below. The typical stress corrosion morphology which was evident in all of the specimens is shown in the SEM micrograph of figure 12a. Figure 12b shows a typical region which has undergone fast fracture. A low magnification SEM micrograph from specimen 28 is shown in figure 13. Note that the fatigue precrack region, the stress corrosion cracking region, and the region of fast fracture is contained within the frame of micrograph extending from left to right. The stress corrosion cracking microstructure can be divided into alternate regions of slow and fast crack growth which correspond to the CMO vs. time curve as shown by the arrows in figure 13. Figure 14 shows the surface of specimen 29 which did not fail during testing. Note the plastic zone associated with local deformation at the crack tip.

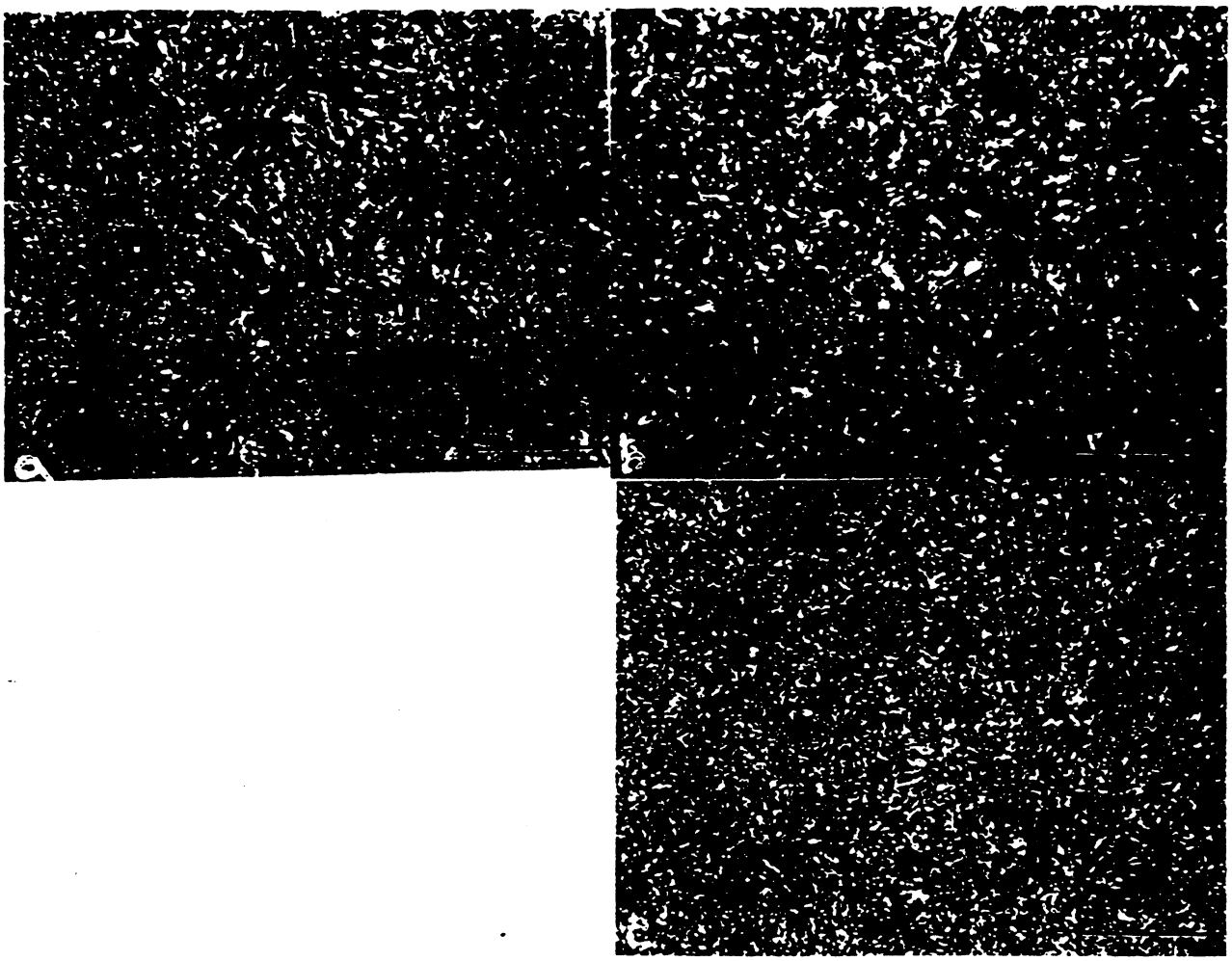

Figure 4. Polished and etched surfaces of the AISI-4340 C(T) specimen from a) parallel to the crack plane. b) perpendicular to the crack plane. c) the C(T) surface.

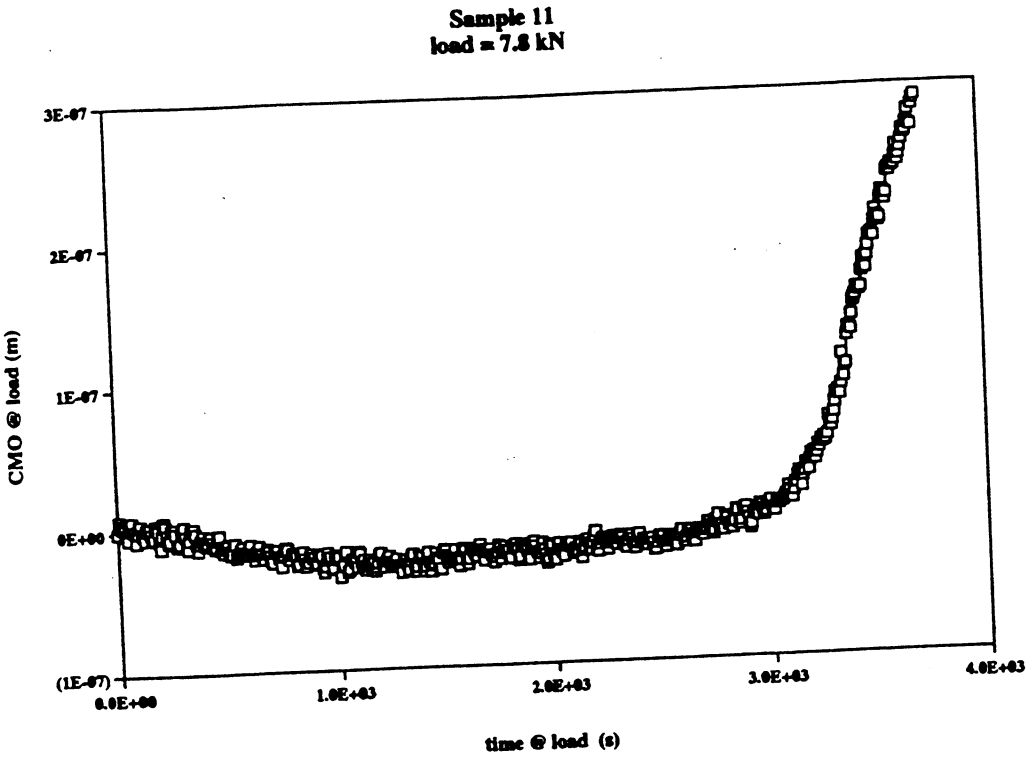

Figure 5. Crack Mouth Opening Displacement vs. time for specimen 11.

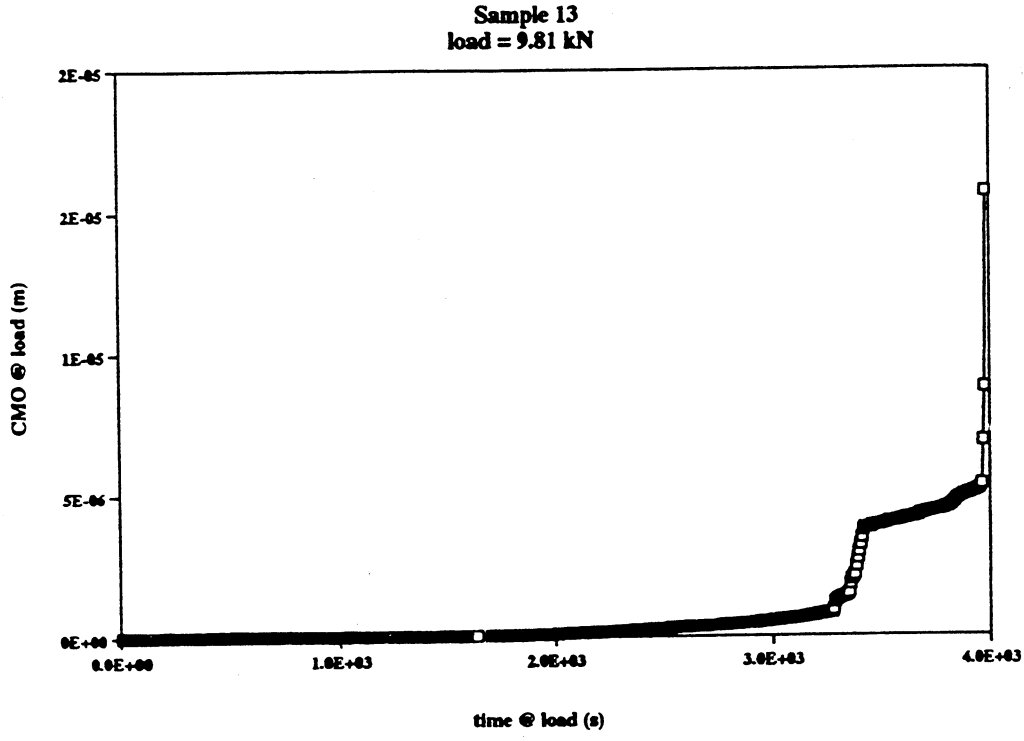

Figure 6. Crack Mouth Opening Displacement vs. time for specimen 13.

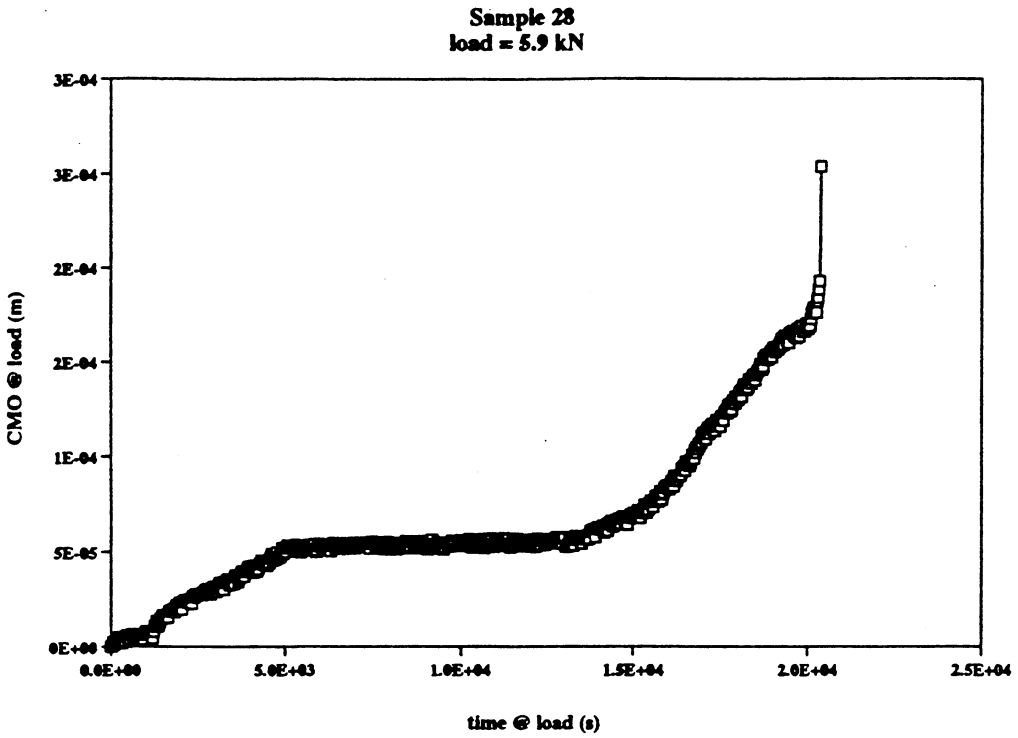

Figure 7. Crack Mouth Opening Displacement vs. time for specimen 28.

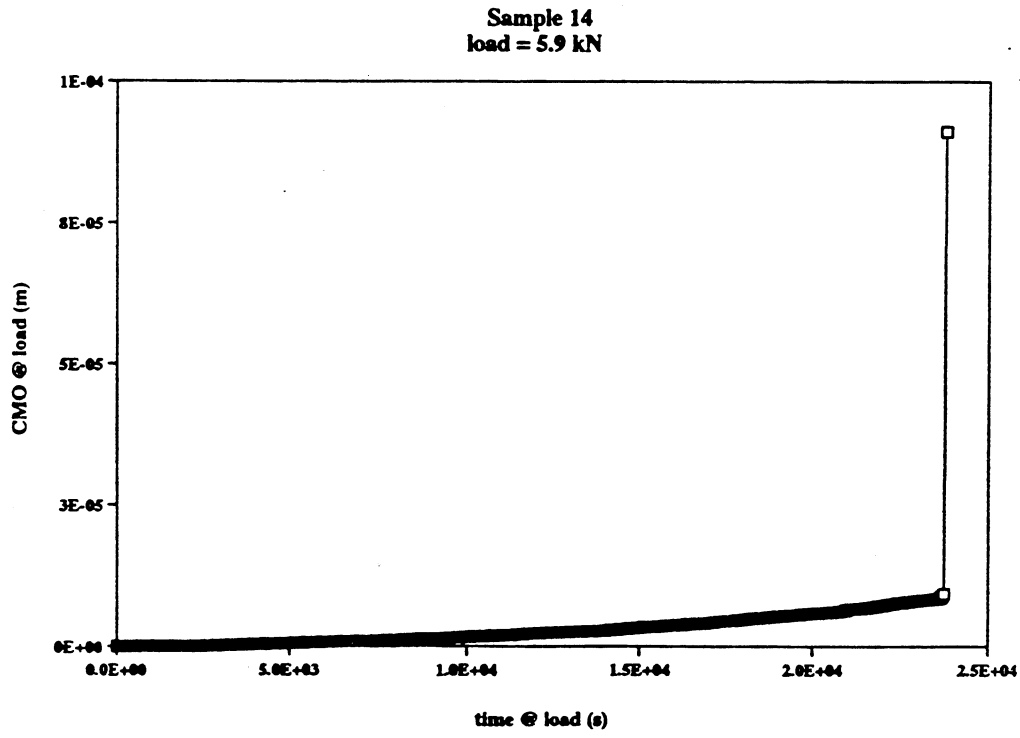

Figure 8. Crack Mouth Opening Displacement vs. time for specimen 14.

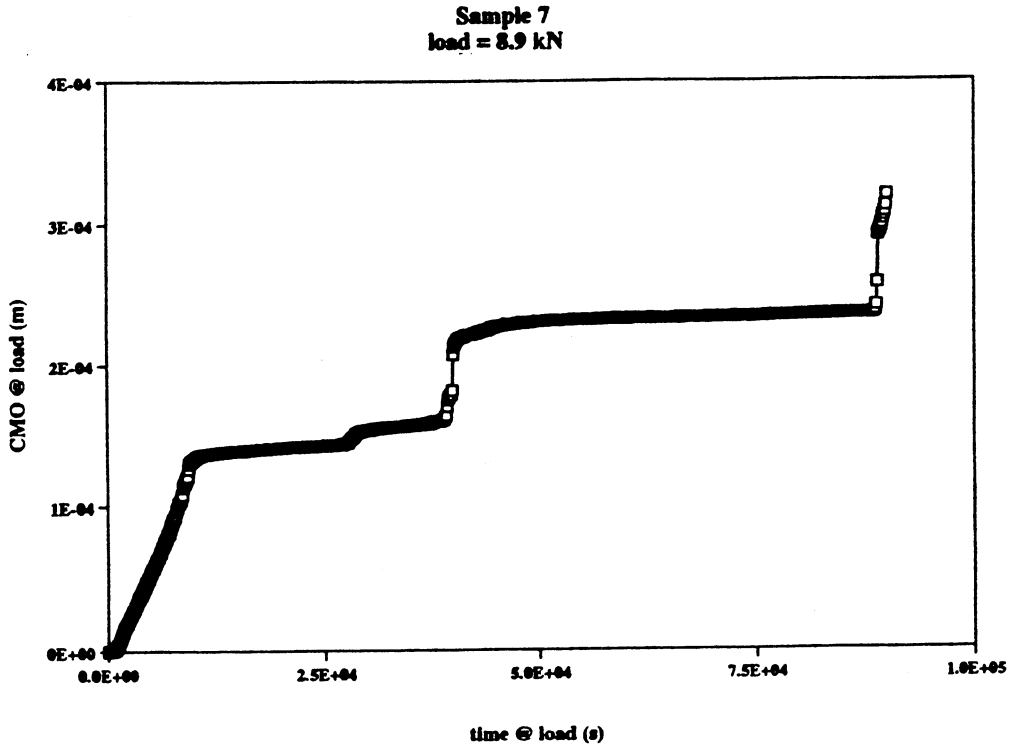

Figure 9. Crack Mouth Opening Displacement vs. time for specimen 7.

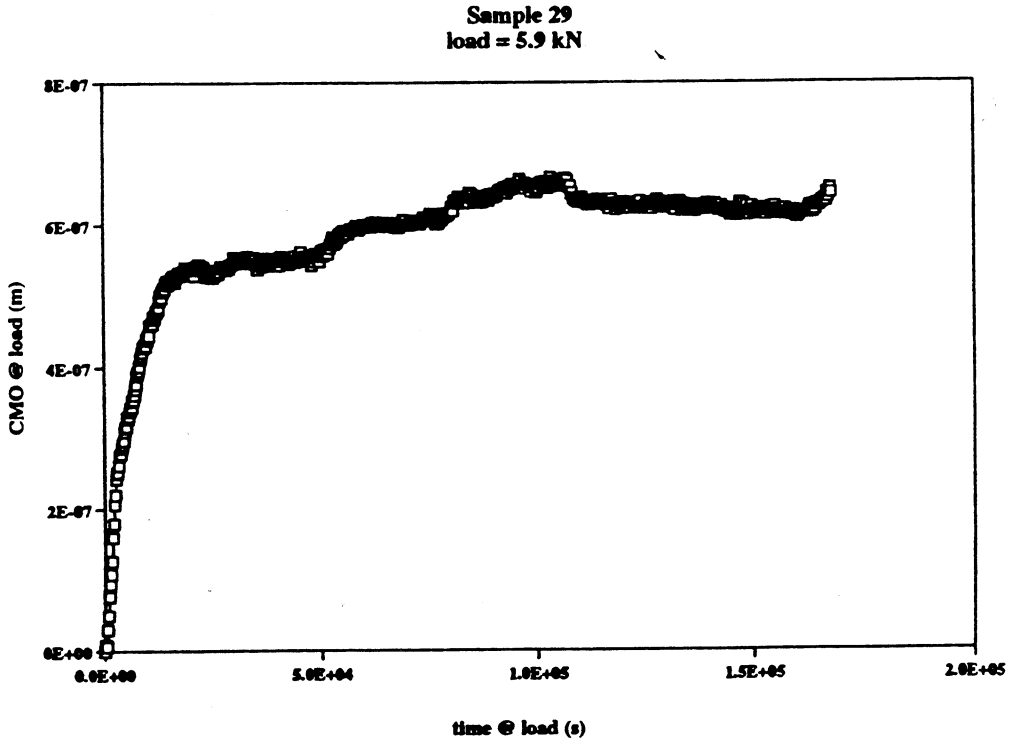

Figure 10. Crack Mouth Opening Displacement vs. time for specimen 29.

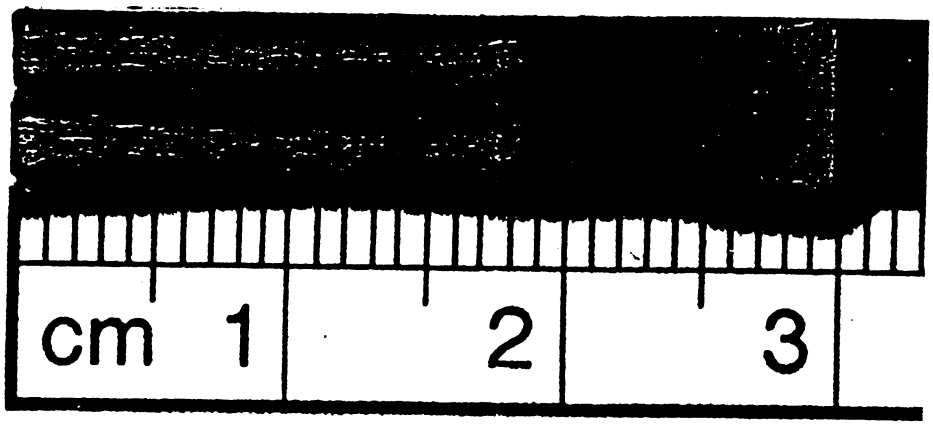

Figure 11. Fracture surface of specimen 13.

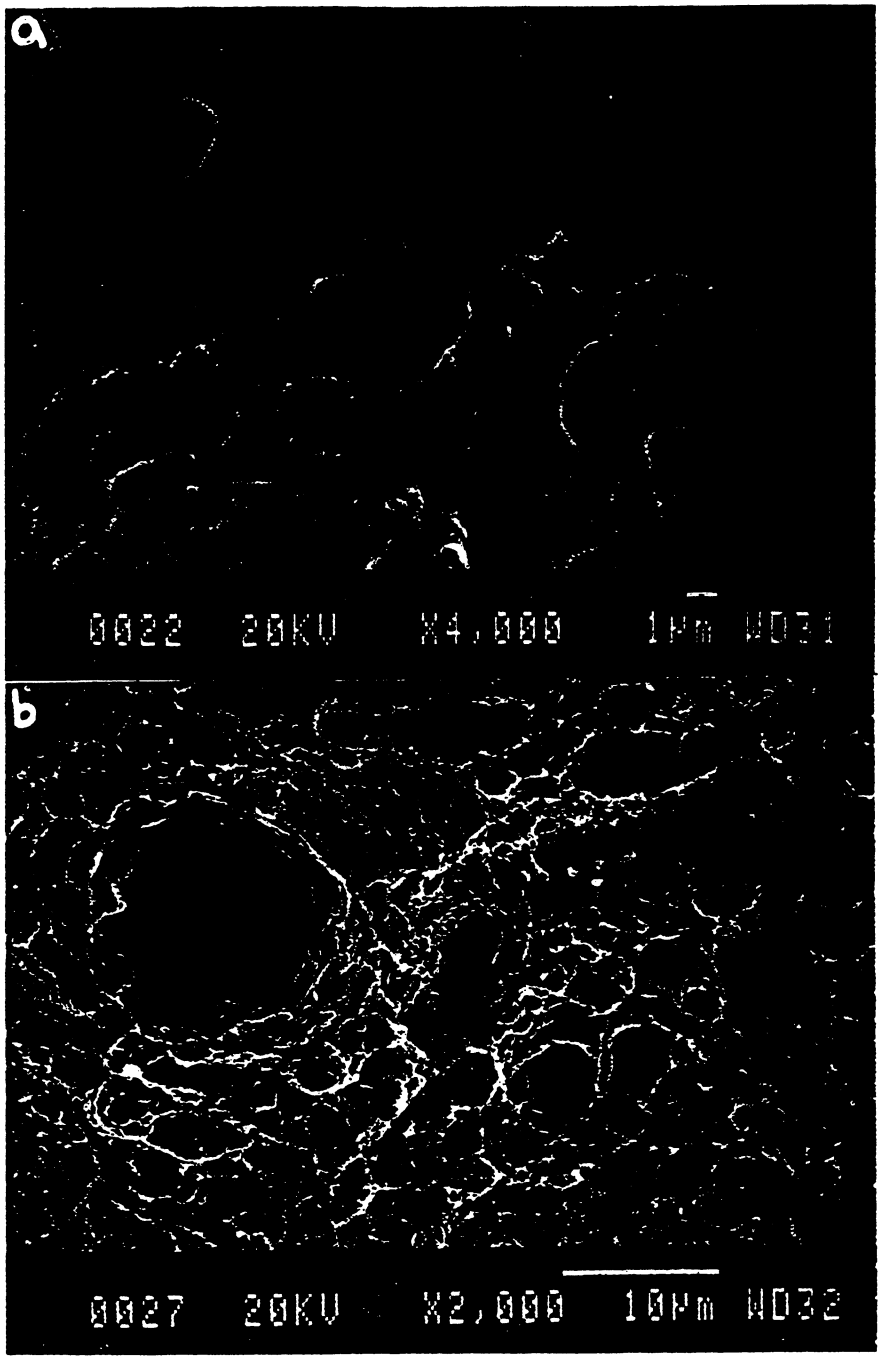

Figure 12. SEM micrograph of a typical SCC fracture surface from: a) the SCC region b) the fast fracture region.

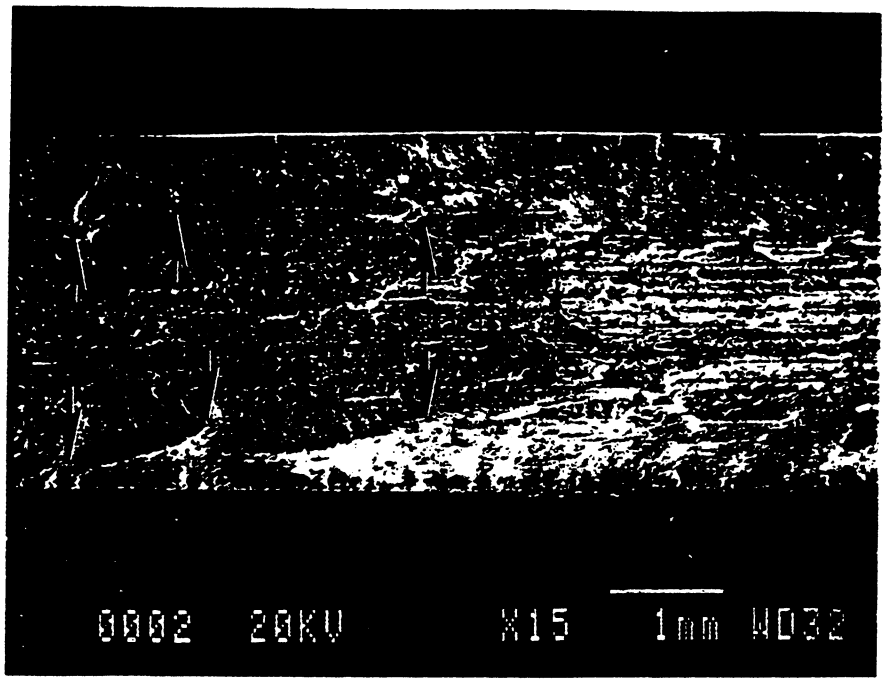

Figure 13. SEM micrograph of the fracture surface of specimen 28.

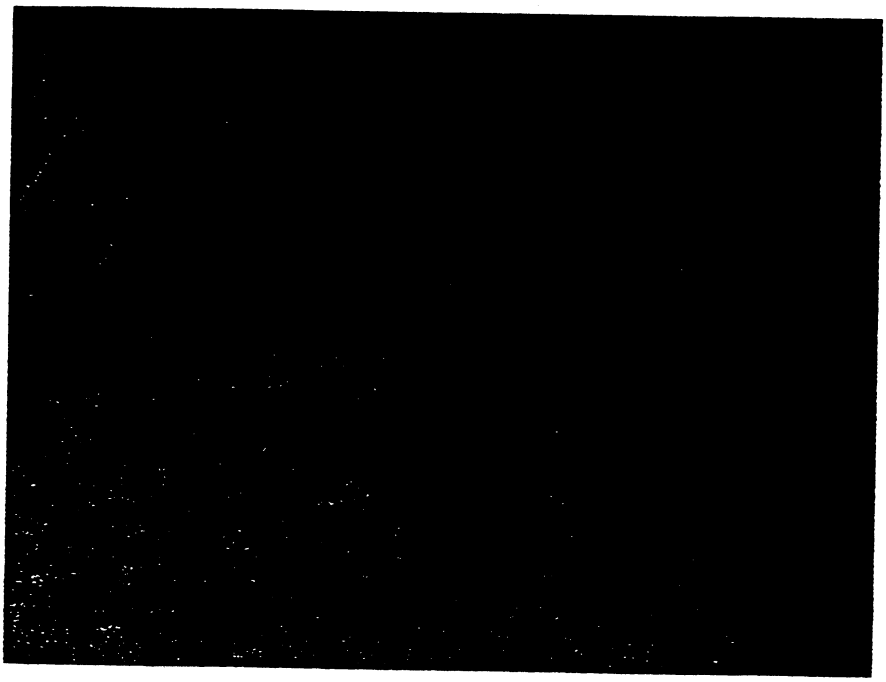

Figure 14. The plastic zone associated with local deformation at the crack tip during crack growth.

IV

CONCLUSIONS

SCC of AISI 4340 steel has been observed during constant loading conditions when exposed to 3.5% NaCl solution. Due to the plane stress conditions which were present during testing, K_{Iscc} and K_{Ic} could not be determined from this study. The crack initiation, nucleation, and growth rates may appear either as a gradual transition as time progresses until failure, or may yield a stepped behavior as time progresses. When a stepped behavior is observed, crack growth rates fluctuate between fast and slow values as K increases, which is not consistent with prior observations where the log(crack growth rate) increases continuously as K increases. Preliminary microstructural analyses of specimen fracture surfaces shows evidence of changing crack growth morphology in regions which are believed to correspond to the stepped crack growth behavior.

REFERENCES

ASM Metals Handbook, 9th ed. vol. 13, (1987), p. 246.

R.A. Davis, "Stress Corrosion Investigation of Two Low Alloy High Strength Steels," Corrosion, 19, 45t-54t, (1963).

R.A. Davis, G.A. Dreyer, and W.C. Gallaugher, "Stress Corrosion Cracking Study of Several High Strength Steels," Corrosion, 20, 93t-103t (1964).

S.W. Dean and H.R. Copson, "Stress Corrosion Behavior of Maraging Nickel Steels in Natural Environments," Corrosion, 21, 95-103 (1965).

E.H. Phelps and A.L. Loginow, "Stress Corrosion of Steels for Aircraft and Missiles," Corrosion, 16, 325t-335t, (1960).

N.A. Tiner and C.B. Gilpin, "Microprocesses in Stress Corrosion of Martensitic Steels," Corrosion, 22, 271-279 (1966).